Journal of Molecular Catalysis B: Enzymatic 71 (2011) 146–151

Contents lists available at ScienceDirect

Journal of Molecular Catalysis B: Enzymatic

journal homepage: www.elsevier.com/locate/molcatb

Direct electron transfer: Electrochemical glucose biosensor based on hollow Pt nanosphere functionalized multiwall carbon nanotubes

Yan Wang, Ruo Yuan*, Yaqin Chaia, Wenjuan Li, Ying Zhuo, Yali Yuan, Jingjing Li

Education Ministry Key Laboratory on Luminescence and Real-Time Analysis, College of Chemistry and Chemical Engineering, Southwest University, Chongqing 400715, People's Republic of China

ARTICLE INFO

Article history:
Received 11 December 2010
Received in revised form 9 March 2011
Accepted 9 April 2011
Available online 15 April 2011

Keywords:
Hollow Pt nanosphere
Direct electron transfer
Multiwall carbon nanotubes
Glucose biosensor

ABSTRACT

Herein, a novel third-generation glucose biosensor based on unique hollow nanostructured Pt decorated multiwall carbon nanotubes (HPt-CNTs) composites was successfully constructed. The HPt-CNTs composites were successfully prepared and cast on the glassy carbon electrode (GCE) surface directly. With the help of electrostatic adsorption and covalent attachment, the negative L-cysteine (L-cys) and the positive poly(diallydimethylammonium) chloride (PDDA) protected gold nanoparticles (PDDA-Au) were modified on the resulting electrode surface subsequently, which provided further immobilization of glucose oxidase (GOD). Exploitation of the unique properties of HPt-CNTs composites led to the achievement of direct electron transfer between the electrode and the redox active centers of GOD, and the electrode exhibited a pair of well-defined reversible redox peaks with a fast heterogeneous electron transfer rate. In particular, the detection limit (4.0×10^{-7} M) of this biosensor was significantly lower and the linear range (1.2 μM–8.4 mM) was much wider than similar carbon nanotubes (CNTs) and Pt-based glucose biosensors. The resulted biosensor also showed high sensitivity and freedom of interference from other co-existing electroactive species, indicating that our facile procedure of immobilizing GOD exhibited better response and had potential application for glucose analysis.

1. Introduction

Direct electrical communication between the redox site of enzymes and the electrodes is a great goal for which researchers have been pursuing recently, because it can establish a desirable and ideal model for the fundamental study of the redox behavior of the enzymes in biological systems [1–4]. Indeed, for enzymes where the redox center is not positioned at the exterior of the protein shell, it has been shown that the electron transfer between the redox center and the electrode is practically prohibited [5–7]. To achieve this communication, nanomaterials have been extensively used in biosensors to actualize the direct electron transfer because of the potentially fast time response and lack of intermediate reactions [8–10]. The latest years have witnessed widely interests in CNTs and hollow nanomaterials for the development of biosensor with high sensitivity and rapid response time [11–13], since they may pierce the glycoprotein shell and effectively shorten the distance between the redox site and the electrode surface. Particularly, Pt nanomaterials with hollow interior appear to be very promising due to their unique capabilities to enhance electron transport, facilitate catalysis, increase surface area and control an electrode's microenvironment [14–17].

Currently, decorating CNTs with metallic nanoparticles to further increase the electrocatalytic activity and biocompatibility of the biosensor offers great potential for electron transfer applications [18–20]. Claussen et al. developed an interesting glucose biosensor comprised of Au-coated Pd nanocubes decorated CNTs with a linear range from 10 μM to 50 mM and a detection limit of 1.3 μM [21]. Decorating CNTs with gold nanoparticles was reported by Rakhi's group [22]. Birkin et al. demonstrated that Pt nanomaterials could be used in combination with CNTs for constructing electrochemical sensors with remarkably improved sensitivity toward H_2O_2 [23]. Results of these biosensors have been very promising for glucose detection, but a scalable fabrication technique is still lacking. Therefore, it is still a challenge to explore new methods or synthesize new matrices to promote the electrical communication between redox sites of enzymes and sensing surface. To the best of our knowledge, the integration of CNTs with hollow Pt nanoparticles is nearly unexplored in biosensor applications, and this could open up a new approach to realize direct electrical communication with redox center of GOD [24–26]. To take full advantages of both the hollow Pt nanoparticles and the CNTs, a new type of catalysts of HPt-CNTs by a two step method was obtained in this study. Ascribing to the presence of more electron-transfer sites or preferential exposure of planes in

* Corresponding author. Tel.: +86 23 68252277; fax: +86 23 68252277.
E-mail address: yuanruo@swu.edu.cn (R. Yuan).

1381-1177/$ – see front matter © 2011 Elsevier B.V. All rights reserved.
doi:10.1016/j.molcatb.2011.04.011

HPt-CNTs catalysts, the HPt-CNTs catalysts decorated biosensors would show perfect biocompatibility, offer a much better electrocatalytic performance and greatly decrease the fabrication time and cost.

Herein, we employed the chitosan (CS) stabilized HPt-CNTs composites as a propellant of direct electron transfer between GOD and the electrode surface, and adopted the PDDA-Au, which can be at relatively high concentrations with predefined size and larger specific surface areas, to fascinate the adsorption of GOD [27]. A mediator-free GOD based glucose biosensor was constructed though a layer-by-layer self-assembly approach. Firstly, the chitosan (CS) stabilized HPt-CNTs composites were successfully modified on the surface of GCE. Then negative charged L-cys was bounded to the resulting electrode, which facilitated the adsorption of positively charged PDDA-Au to the electrode. Finally, the GOD was self-assembled on the large and specific surface of PDDA-Au. The biosensor exhibited specific and sensitive detection for glucose with wide linear range, short response time, low detection limit and high sensitivity. Preparation, characterization, performance and factors influencing the performance of the obtained biosensor were investigated in detail as described in the next section.

2. Experimental

2.1. Reagents

The multiwall carbon nanotubes (MWCNTs > 95% purity) were obtained from Chengdu Organic Chemicals Co., Ltd. of the Chinese Academy of Science (Chengdu, China). Chloroplatinic acid (H_2PtCl_6) were bought from Chongqing Chemical Reagent Co. (Chongqing, China), gold chloride ($HAuCl_4$), $NaBH_4$ and glucose oxidase (E.C. 1.1.3.4, 151,000 unit/g), poly(diallyldimethylammonium chloride) (PDDA, MW: 200,000–350,000), chitosan (CS, MW: 100,000–300,000, deacetylating grade: 70–85%) were all purchased from Sigma Chemical Co. (St. Louis, MO, USA), L-cysteine (L-cys) was purchased from Kangda Amino Acid (Shanghai, China). Glucose was obtained from Sinopharm Chemical Reagent Co., Ltd. (Shanghai, China) and glucose stock solution was stored at room temperature for 24 h before using to mutarotate. Poly(vinylpyrrolidone) (PVP, MW = 40,000), $CoCl_2{\cdot}6H_2O$, $K_3[Fe(CN)_6]$ and other chemicals were of analytical grade and purchased from Beijing Chemical Reagent Co. (Beijing, China), Phosphate buffer saline (PBS) with various pH values was prepared with stock standard solutions of 0.1 M KH_2PO_4 and 0.1 M K_2HPO_4. Double distilled water was used throughout.

2.2. Apparatus and measurements

Amperometric experiments and cyclic voltammetric experiments were performed on a CHI 660A electrochemical work station (Shanghai CH Instruments Co., China). A conventional three electrode system was applied, composing of a modified electrode as working electrode, a platinum wire as auxiliary electrode, and a saturated calomel electrode (SCE) as reference electrode. All potentials were measured and reported versus the SCE. Transmission electron microscopy (TEM) was carried out on a TECNAI 10 (PHILIPS FEI Co., Holland). All the electrochemical experiments were carried out at room temperature.

2.3. Preparation of HPt-CNTs composites

Initially, MWCNTs were purified by using acid treatment [28]. A HPt-CNTs catalyst was prepared by a two-step method according to the literature [16] with a slight change. Briefly, $CoCl_2{\cdot}6H_2O$ (5.6 mg) and PVP (100 mg) were dissolved in 50 mL double distilled water, sonicated for 15 min to dissolve fully. After purged with N_2 for 15 min, a freshly prepared $NaBH_4$ (15 mM) was added dropwise into the solution under vigorous stirring. Immediately after all of the $NaBH_4$ had been added, 12 mL of H_2PtCl_6 (0.1%) was added dropwise with stirring. The color of the solution became blackish brown gradually, which showed that a trans-metallation reaction occurred. The Co nanoparticles were oxidized to Co^{2+} ions by $PtCl_6^{2-}$ according to the equation as follows [15]:

$$2Co + PtCl_6^{2-} = Pt + 2Co^{2+} + 6Cl^-$$

After cobalt element was completely oxidized by slightly excessive $PtCl_6^{2-}$, MWCNTs supports (12 mg dispersed in 6 mL H_2O) were then added to the above solution. The product was collected by centrifugation 3 h later, and washed several times with double distilled water and ethanol. Finally, 4 mg of the HPt-CNTs composites were dispersed in 1 mL 0.2% of CS (1% acetic acid), sonicated until to form homogeneous blackish solution for further use. For comparison, the SPt-CNTs catalysts were directly synthesized by adding $NaBH_4$ solution into H_2PtCl_6 solution with the same amount of MWCNTs.

2.4. Preparation of PDDA-Au nanoparticles

In a typical experiment, 250 μL PDDA (4 wt.% in water), 40 mL double distilled water, 200 μL 0.5 M NaOH and 100 μL $HAuCl_4$ (1%) were added into a beaker according to the literature [29]. After thoroughly mixed for a few minutes, heat the mixed solution to boiling for several minutes until the color of the solution changed to red and no further color change occurred.

2.5. Fabrication of the glucose biosensor

The assembly process of the electrode was described in Scheme 1. Before each modification, the glassy carbon electrode (GCE) was polished successively with 0.3 and 0.05 μm alumina to produce a smooth, shiny surface, then rinsed thoroughly with distilled water, followed by an ultrasonic bath in ethanol and twice-distilled water for 5 min, respectively. Subsequently, 8 μL of the HPt-CNTs-CS suspension was coated onto the pretreated GCE and dried in the air. Then the electrode was immersed in L-cys (20 mM pH 6.5) for 5 h and PDDA-Au solution for 8 h respectively. Having been rinsed thoroughly with distilled water to remove some weakly adsorbed species, the electrode was dipped in GOD solution (10 mg mL^{-1} pH 7.0) overnight to attach enzyme molecules. For a comparative purpose, a similar kind of electrode modification was performed using SPt-CNTs-CS suspension. The modified electrodes were stored at 4 °C when not in use.

3. Results and discussion

3.1. Characterizations of the HPt-CNTs and SPt-CNTs composites

The morphological features of the HPt-CNTs and SPt-CNTs composites were investigated by transmission electron microscopy (TEM). Fig. 1(a) showed a typical TEM image of SPt-CNTs composites, it could be seen that Pt nanoparticles dispersed well on the surface of MWCNTs were solid, with a diameter ranging form 2–6 nm. Fig. 1(b) presented the information of the HPt-CNTs composites, it was found that several hollow Pt nanospheres were obtained, which were composed of an empty interiors with a perfect Pt shell, that is, a hollow structure. These hollow Pt nanospheres seemed to be porous and consisted of tiny solid Pt nanoparticles, and they firmly glued to the surface of MWCNTs. Thus, compared to the solid Pt nanoparticles, the large pore volume inside the hollow nanospheres endows the hollow Pt nanoparticles with higher surface area.

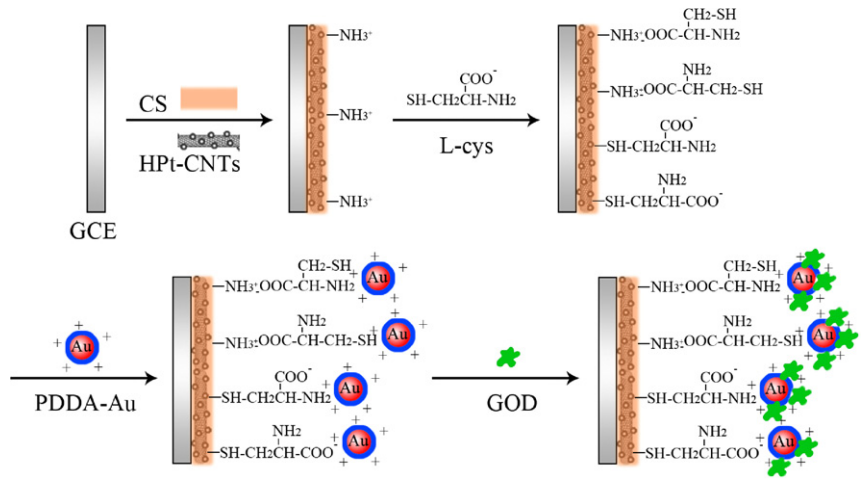

Scheme 1. The illustration of the stepwise fabrication process of the biosensor.

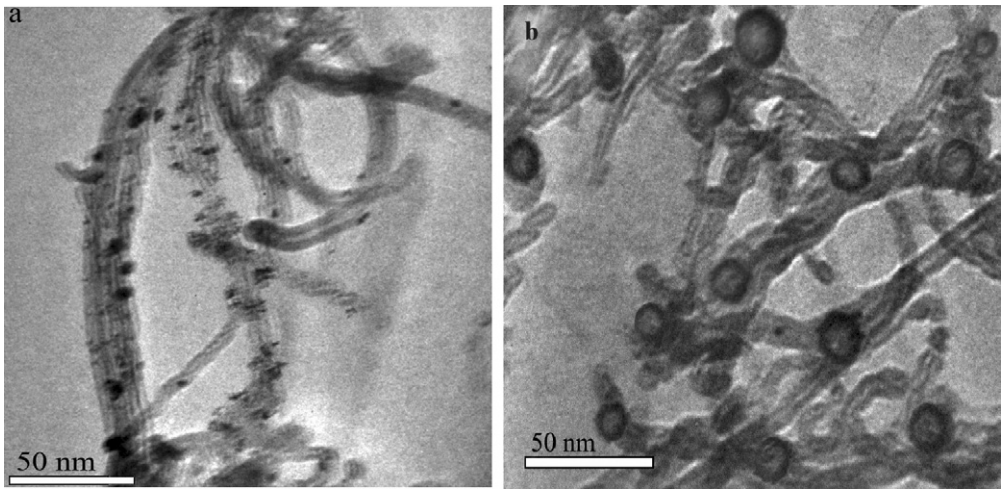

Fig. 1. TEM images of the solid Pt supported MWCNTs composites (a) and hollow Pt supported MWCNTs composites (b).

3.2. Electrochemical characteristics of the modified electrode

CV of the ferricyanide system is a convenient and valuable tool to monitor the characteristics of the surface of each modified electrode. The CVs of the fabricated biosensor during stepwise modification conducted in 5 mM $K_3Fe(CN)_6$ with a scan rate of 50 mV/s were shown in Fig. 2A. As can be seen, a well-defined oxidation and reduction peak of $[Fe(CN)_6]^{3-/4-}$ was observed at the bare electrode (a). Curve b showed the HPt-CNTs-CS film modified electrode, the peak current increased markedly, indicating

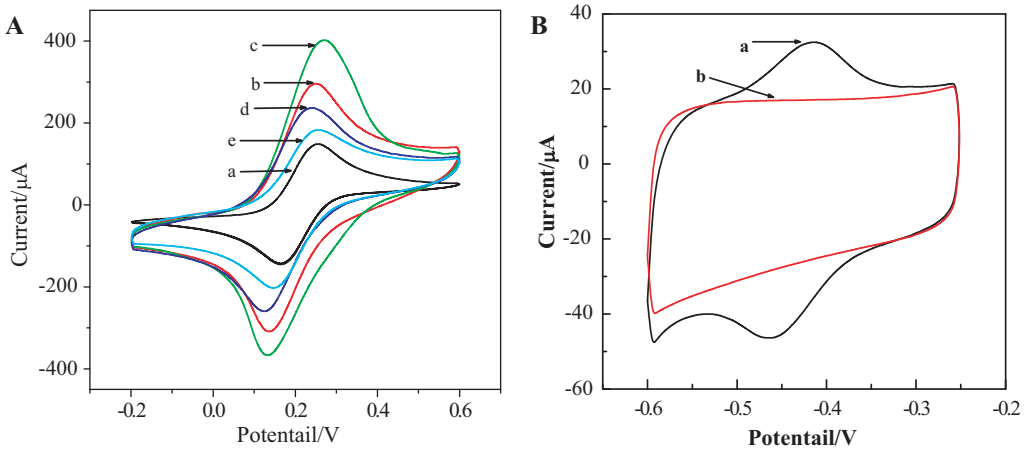

Fig. 2. (A) CVs of bare GCE (a); GCE/HPt-CNTs-CS (b); GCE/HPt-CNTs-CS/L-cys (c); GCE/HPt-CNTs-CS/L-cys/PDDA-Au (d); GCE/HPt-CNTs-CS/L-cys/PDDA-Au/GOD (e) in 5 mM $[Fe(CN)6]^{4-/3-}$, Scan rate: 50 mV/s. (B) CVs of GCE/HPt-CNTs-CS/L-cys/PDDA-Au/GOD (a); GCE/HPt-CNTs-CS/L-cys/PDDA-Au (b) in 0.1 M PBS (pH 7.0), Scan rate: 50 mV/s.

that hollow Pt functioned MWCNTs could promote the electron transfer. When L-cys were adsorbed onto the electrode, the current increased sharply(c), suggesting that the L-cys had greatly facilitated the electron transfer of the biosensor. After modified with the non-conductive PDDA-Au, a large decrease in peak current was observed (d), indicating that the L-cys had facilitated the adsorption of positively charged PDDA-Au onto the surface. When the GOD was assembled on the electrode (e), the peak current clearly decreased, implying that the non-conductive GOD was successfully modified on the electrode.

In order to verify the large adsorption of GOD on the electrode, a further CV study was performed at the GOD/PDDA-Au/L-cys/HPt-CNTs-CS (a) and PDDA-Au/L-cys/HPt-CNTs-CS (b) modified electrode respectively. As we can see in Fig. 2.B, neither oxidation nor reduction occurred on the PDDA-Au/L-cys/HPt-CNTs-CS/GCE, however, after modified with GOD, the electrode presented a pair of well defined redox peaks (Epa = −0.415 V, Epc = −0.465 V, the formal potential = −0.44 V, curve a), and the peak current of the GOD increased 16.3 μA, indicating the enzyme loading was large enough to support readily detectable redox currents. This mainly due to the abundant electron-transfer sites and high surface area of HPt-CNTs catalysts and PDDA-Au, which could offer special opportunities for the adsorption and entrapment of GOD.

3.3. Effect of pH value and applied potential on the response current of the biosensor

The effect of pH value on the performance of the biosensor is of great consequence since the activity of the immobilized GOD is pH dependent. Fig. 3.A showed the response current of the enzyme electrode in a series of PBS with the pH from 4.5 to 8.5 in glucose solution (0.1 mM), the response current showed the maximum value at pH 7.0, Therefore, pH 7.0 was chosen for the detection of glucose.

To determine the optimum applied potential for the biosensor operation, amperometric measurements were carried out in 0.1 M PBS containing 0.1 mM glucose. The biosensor was operated at a different potential changing from 0 to 0.6 V (with 0.05 V potential step), and the transient currents were permitted to attenuate to a steady-state value. As can be seen from Fig. 3B, the current response of the biosensor increased with the change of applied potential from 0 to 0.6 V. Given the risk of interfering reactions of the other electroactive species at higher potential, we chose 0.4 V as the optimum applied potential. Because the biosensor can maintain higher sensitivity and minimize the risk of interferences from other electroactive species.

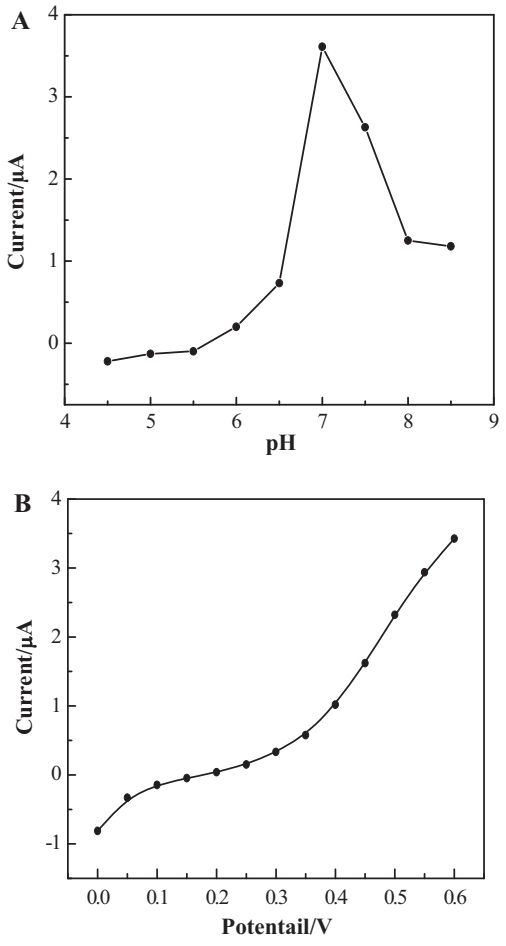

Fig. 3. Dependence of the current change of biosensor to 0.5 mM glucose on the pH of buffer solutions at an applied potential of 0.4 V (A) and the applied potential in 0.1 M PBS (pH 7.0) (B).

3.4. Chronoamperometric response

3.4.1. Amperometric response of hydrogen peroxide and glucose of different electrodes

As well known, the quantification of glucose can be achieved via electrochemical detection of the enzymatically liberated H_2O_2. Therefore, a series of experiments were performed to determine the electrochemical response of H_2O_2 at the HPt-CNTs-CS composites, SPt-CNTs-CS composites and CNTs-CS composites modified electrodes respectively. As shown in Fig. 4A, the conventional CNTs-CS film modified electrode (a) generated very small response, while the SPt-CNTs-CS composites modified electrode (b) gave a increase of oxidation current. However, compared to the SPt-CNTs-CS composites modified electrode, an obvious improvement in current at HPt-CNTs-CS composites (c) were obtained in the same condition. This increase, we believe, was attributed to the outstanding surface area and abundant electron-transfer sites of HPt-CNTs catalysts.

In order to check the catalytic performance of the hollow and solid Pt nanoparticles modified electrodes, a comparative study at the applied potential with injecting the same amount of glucose was carried out by adopting two kinds of different modified biosensors: (a) GOD/PDDA-Au/L-cys/ SPt-CNTs-CS/GCE, (b) GOD/PDDA-Au/L-cys/HPt-CNTs-CS/GCE. As shown in Fig. 4B, it can be found that the current response of the GOD/PDDA-Au/L-cys/HPt-CNTs-CS/GCE was about five times higher than that of GOD/PDDA-Au/L-cys/SPt-CNTs-CS/GCE at the same condition, the response time was faster and the linear range was much wider too. These results demonstrated that the elegantly simple physicochemical adsorption of GOD to the surface of HPt-CNTs and PDDA-Au resulted in direct electron transfer, facilitating the substrate-enzyme contact, thus helped to increase the sensitivity and expand the linear range.

3.4.2. Chronoamperometric response and calibration curve

We used the steady-state current to plot with the concentration of glucose. Fig. 5 represented the typical current-time response of the GOD/PDDA-Au/L-cys/HPt-CNTs-CS/GCE biosensor on successive step changes of glucose concentration under the optimized experimental conditions. With the increase of the concentration of glucose, the responded current increased rapidly. There was an excellent linear relation of the current to concentration of glucose from 1.2 μM to 8.4 mM with a correlation coefficient of 0.996, as shown in the inset of Fig. 5 A. The linear regression equation was i (μA) = 4.79 C (glucose, mM) +1.6632. The dynamic curve showed a remarkable sensitivity of 20.1 $mAM^{-1}\,cm^{-2}$ with a detection limit of 4×10^{-7} M at the signal-to-noise ratio of 3. The obtained biosen-

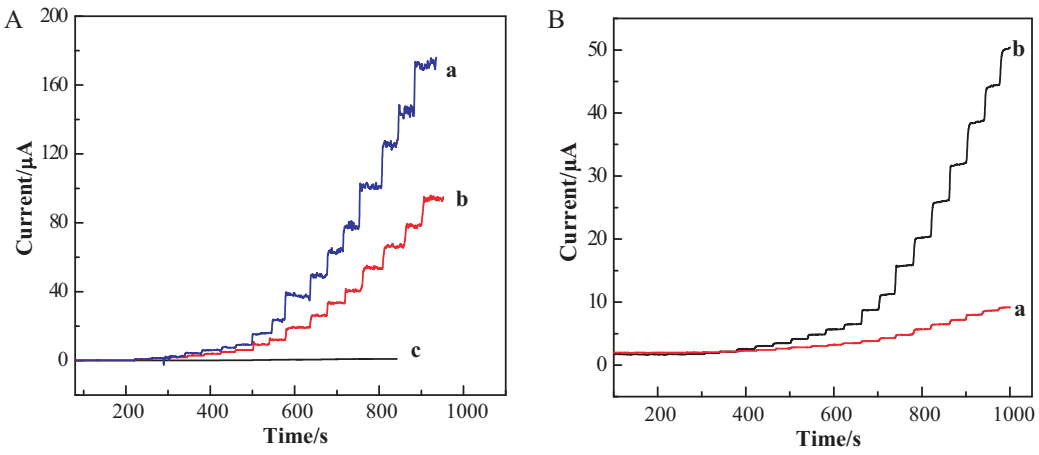

Fig. 4. (A) Current–time recording obtained upon successive injection of different concentration of H_2O_2 into a stirred solution at the GCE modified with (a) HPt-CNTs-CS composites; (b) SPt-CNTs-CS composites; (c) MWCNTs-CS composites. (B) Current–time response for the biosensor upon the successive addition of glucose into a stirred solution for GOD/PDDA-Au/L-cys/SPt-CNTs-CS/GCE (a), GOD/PDDA-Au/L-cys/HPt-CNTs-CS/GCE (b).

sor achieved 95% of the steady-state current within 5 s. The current tended to reach at a saturation value at high glucose concentration, showing the characteristics of the Michaelis–Menten kinetics (Fig. 5B). According to Lineweaver–Burk equation [30], the value of K_m^{app} was estimated to be 4.14 mM, which indicated that the immobilized GOD on the electrode possessed higher enzymatic activity.

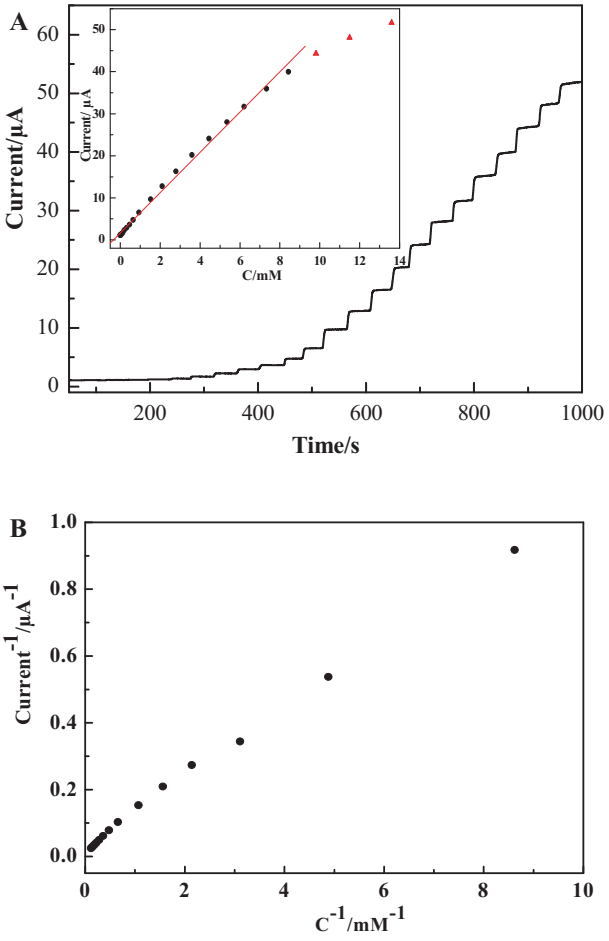

Fig. 5. (A) Amperometric response of the biosensor in stirred solutions to the successive additions of glucose in 0.1 PBS (pH 7.0). The inset shows linear calibration curves. (B) The Lineweaver–Burk plot for measurement of the apparent Michaelis–Menten constant K_m^{app}

Additionally, the results of the developed glucose biosensor had been compared with other glucose biosensors listed in Table 1. As can be seen, the comparative data suggested that this biosensor exhibited excellent performance in terms of linearity range, detection limit and response time. We believed that the exploitation of HPt-CNTs composites and PDDA-Au could dramatically increase the adsorption of GOD, which allowed to pierce the glycoprotein shell of the GOD and gained access to the redox sites within tunnelling distance. This then would permit direct electron transfer, which could effectively reduce response time, enlarge linearity range and enhance the sensitivity.

3.5. Reproducibility and stability of the glucose biosensor

The reproducibility is an important parameter for evaluation of the performance of the biosensor, which was evaluated from the response to 0.6 mM glucose at five electrodes fabricated at the same condition. The results revealed that the biosensor showed good reproducibility with a relative standard deviation (RSD) of 4.7%. Additional experiments were carried out to test the stability over a period of 3 weeks, which was tested in 0.6 mM glucose solution every week, and the electrode was kept at 4 °C in a refrigerator. The results showed that the biosensor lost only 5.3% of the initial response after one weeks and the catalytic current response maintained more than 83.7% of its initial value after storage for 3 weeks. The decreased current might be attributed to the possible leakage of weakly bound GOD to the PDDA-Au, which reduced the performance of the biosensor in the oxidation process.

3.6. Interference determination

In real samples some co-existing electroactive species (such as ascorbic acid, L-cysteine) might cause problems in accurate determination of glucose. In our experiment, the effect was tested by adding five interferents (dopamine, glycin, L-cysteine, ascorbic acid and ethanol) to the glucose solution. The biosensor was kept in a stirred solution of 0.1 M PBS (pH 7.0). A 0.5 mM glucose solution was added firstly, then, 1 mM ethanol, 1 mM glycin, 1 mM L-cysteine, 1 mM ascorbic acid and 1 mM dopamine were added sequentially, after that 1 mM glucose was added again, which was indicated by arrows in Fig. 6. These results indicated that above five tested interferents only resulted in a very negligible increase in the background signal, suggesting that the direct electron transfer between redox proteins and electrodes of this biosensor helped to avoid the intermediate reactions that could cause interference.

Table 1
Comparison of the performance of different glucose biosensors.

Biosensor fabrication	Linear range (mM)	Detection limit (μM)	K_m^{app} (mM)	Response time(s)	Ref.
GCE/MWCNTs/Pt/GOD-CS–SiO_2	0.001–23.0	1.0	14.4	<5	[31]
GCE/CS/FeyOx-MWCNTs/Pt/GOD/Nafion	0.006–6.2	2.0	9.0	<8	[32]
CNTs/PtNP/CH-MTOS/GOD	0.0013–6.0	0.3	7.9	5	[33]
AuE/ACNTs/PtNPs/ GOD/Nafion	0.01–7.0	8.89	9.28	<5	[34]
GCE/ACS /Pt-MWCNT/GOD	50–10.05	6.18	11.02	<5	[35]
TiO_2/CNT/Pt/GOD	0.006–1.5	5.7	–	<3	[36]
GCE/CS–PB@MWCNTs/H-PtCo/GOD/Nafion	0.003–3.6	0.85	–	<8	[37]
GCE/HPt-CNTs-CS/L-cys/PDDA-Au/GOD	0.0012–8.4	0.4	4.14	<5	This work

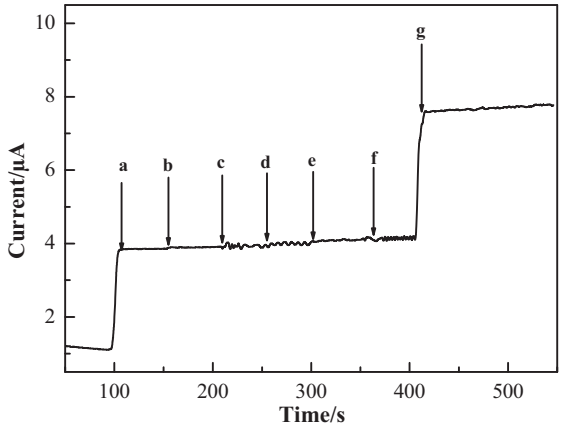

Fig. 6. Effect of the possible interferents in glucose biosensors. The arrows show the moment at the injection of each interfering compounds: (a) 0.5 mM glucose; (b) 1 mM ethanol; (c) 1 mM glycin; (d) 1 mM l-L-cysteine; (e) 1 mM ascorbic acid; (f) 1 mM dopamine; (g) 1 mM glucose.

4. Conclusions

An electrochemical glucose biosensor of high selectivity and good sensitivity with the employment of HPt-CNTs composites and PDDA-Au has been successfully demonstrated in this work. The HPt-CNTs nanocomposites increased the effective electrode surface area and PDDA-Au served as an excellent support for the further immobilizing of GOD. The resulted biosensor exhibited superior performance such as low detection limit, wide linear range, rapid response time and satisfactory sensitivity. This enhancement was attributed to a number of factors, including the controlled highly sensitive surface area, the low electrical resistance pathway at the HPt-CNTs interface, the selective enzyme adhesion and direct electron transfer that occured between the GOD and HPt-CNTs interfaces. We believe that the performance of this approach will be useful for adaptation to a microbiosensor format and could be used as a tool for biomedical research in biosensing applications.

Acknowledgements

The authors are grateful for the financial supports provided by the NNSF of China (20675064), the Ministry of Education of China (Project 708073), the Natural Science Foundation of Chongqing City (CSTC-2009BA1003) and High Technology Project Foundation of Southwest University (XSGX02), China.

References

[1] C. Fan, K.W. Plaxco, A.J. Heeger, J. Am. Chem. Soc. 124 (2002) 5642–5643.
[2] Y. Tian, L. Mao, T. Okajima, T. Ohsaka, Anal. Chem. 74 (2002) 2428–2434.
[3] B.A. Kuznetsov, G.P. Shumakovich, O.V. Koroleva, A.I. Yaropolov, Biosens. Bioelectron. 16 (2001) 73–84.
[4] M. Tasviri, H. Rafiee-Pour, H. Ghourchian, M.R. Gholami, J. Mol. Catal. B: Enzyme 68 (2011) 206–210.
[5] K.Q. Wang, H. Yang, L. Zhu, J.H. Liao, T.H. Lu, W. Xing, S.Y. Xing, Q. Lv, J. Mol. Catal. B: Enzyme 58 (2009) 194–198.
[6] C.B. Jacobs, M.J. Peairs, B.J. Venton, Anal. Chim. Acta 662 (2010) 105–127.
[7] C.X. Cai, J. Chen, Anal. Biochem. 332 (2004) 75–83.
[8] Y. Xiao, F. Patolsky, E. Katz, J.F. Hainfeld, I. Willner, Science 299 (2003) 1877–1881.
[9] P. Karam, Y. Xin, S. Jaber, L.I. Halaoui, J. Phys. Chem. C 112 (2008) 13846–13850.
[10] L. Bahshi, M. Frasconi, R. Tel-Vered, O. Yehezkeli, I. Willner, Anal. Chem. 80 (2008) 8253–8259.
[11] S.H. Lee, T.T.N. Doan, K. Wonc, S.H. Ha, Y.M. Koo, J. Mol. Catal. B: Enzyme 62 (2010) 169–172.
[12] Y. Liu, M. Wang, F. Zhao, Z. Xu, S.J. Dong, Biosens. Bioelectron. 21 (2005) 984–988.
[13] J. Wang, M. Musameh, Y. Lin, J. Am. Chem. Soc. 125 (2003) 2408–2409.
[14] C.Y. Wang, S.H. Chen, Y.X., W.J. Li, X.Z., X. Che, J.J. Li, J. Mol. Catal. B: Enzyme 69 (2011) 1–7.
[15] H.P. Liang, H.M. Zhang, J.S. Hu, Y.G. Guo, L.J. Wan, C.L. Bai, Angew. Chem. Int. Ed. 116 (2004) 1566–1569.
[16] Y. Vasquez, A.K. Sra, R.E. Schaak, J. Am. Chem. Soc. 127 (2005) 12504–12505.
[17] X.Q. Huang, H.H. Zhang, C.Y. Guo, Z.Y. Zhou, N.F. Zheng, Angew. Chem. Int. Ed. 48 (2009) 4808–4812.
[18] S. Hrapovic, Y. Liu, K.B. Male, J.H.T. Luong, Anal. Chem. 76 (2004) 1083–1088.
[19] S.H. Lim, J. Wei, J. Lin, Q. Li, J. KuaYou, Biosens. Bioelectron. 20 (2005) 2341–2346.
[20] H. Tang, J. Chen, S. Yao, L. Nie, G. Deng, Y. Kuang, Anal. Biochem. 331 (2004) 89–97.
[21] J.C. Claussen, A.D. Franklin, A. Haque, D.M. Porterfield, T.S. Fisher, ACS Nano 3 (2009) 37–44.
[22] R.B. Rakhi, K. Sethupathi, S. Ramaprabhu, J. Phys. Chem. B 113 (2009) 3190–3194.
[23] P.R. Birkin, J.M. Elliot, Y.E. Watson, Chem. Commun. 17 (2000) 1693–1694.
[24] S. Hrapovic, E. Majid, Y. Liu, K. Male, J.H.T. Luong, Anal. Chem. 78 (2006) 5504–5512.
[25] J.N. Xie, S. Wang, L. Aryasomayajula, V.K. Varadan, Nanotechnology 18 (2007) 065503–065511.
[26] X.W. Lou, L.A. Archer, Z. Yang, Adv. Mater. 20 (2008) 3987–4019.
[27] D.I. Gittins, F. Caruso, Angew. Chem. Int. Ed. 16 (2001) 3001–3004.
[28] M.L. Guo, J.H. Chen, L.H. Nie, S.Z. Yao, Electrochim. Acta 49 (2004) 2637–2643.
[29] S.C. Mu, H.L. Tang, Z.H. Wan, M. Pan, R.Z. Yuan, Electrochem. Commun. 7 (2005) 1143–1147.
[30] R.A. Kamin, G.S. Wilson, Anal. Chem. 52 (1980) 1198–1205.
[31] Y.J. Zou, C.L. Xiang, L.X. Sun, F. Xu, Biosens. Bioelectron. 23 (2008) 1010–1016.
[32] J.J. Li, R. Yuan, Y.Q. Chai, X. Che, J. Mol. Catal. B: Enzyme 66 (2010) 8–14.
[33] X. Kang, Z. Mai, X. Zou, P. Cai, J. Mo, Talanta 74 (2008) 879–886.
[34] K. Zhao, S.Q. Huang, Z. Chang, H.Y. Songm, L.M. Dai, P.G. He, Y.Z. Fang, Electroanalysis 19 (2007) 1069–1074.
[35] M.C. Tsai, Y.C. Tsai, Sens. Actuators B 141 (2009) 592–598.
[36] X.Y. Pang, D.M. He, S.L. Luo, Q.Y. Cai, Sens. Actuators B 137 (2009) 134–138.
[37] X. Che, R. Yuan, Y.Q. Chai, J.J. Li, Z.J. Song, W.J. Li, Electrochim. Acta 55 (2010) 5420–5427.